WILEY-VCH

DOI: 10.1002/ ((please add manuscript number))
Article type: Full Paper

Direct simulation of ternary mixture separation in a ZIF-8 membrane at molecular scale

*Sadanandam Namsani, Aydin Ozcan and A. Ozgur Yazaydin**

Dr S. Namsani, A. Ozcan, Prof A. O. Yazaydin
Department of Chemical Engineering, University College London, Torrington Place, London, WC1E 7JE, United Kingdom.
E-mail: ozgur.yazaydin@ucl.ac.uk

Keywords: Non-equilibrium molecular dynamics, Ternary mixture separation, permselectivity, membrane separation

Separation of H_2 in a ZIF-8 membrane from a syngas mixture composed of CO_2, H_2 and N_2 at 300K and 35 atm is simulated with the concentration gradient driven molecular dynamics (CGD-MD) method. Steady-state fluxes are computed to predict the H_2 selectivity of the ZIF-8 membrane using four different flexible force fields developed for ZIF-8. The permselectivities predicted by the CGD-MD method are compared with those obtained from the GCMC+EMD approach, which is based on the solution-diffusion model and widely used to predict permselectivities for mixture separations. The permselectivities obtained by using the CGD-MD method accurately predict that ZIF-8 is H_2 selective over CO_2 and N_2. On the other hand, permselectivities predicted with the GCMC+EMD approach are found to be incorrect, i.e. ZIF-8 not selective for H_2. Our study suggests that a reliable non-equilibrium molecular dynamics approach should be employed in order to obtain accurate predictions for the permselectivity of a membrane for a multicomponent mixture separation process which happens at moderate or high pressures conditions.

1. Introduction

Porous membranes are widely used for the separation of mixtures in the gas or liquid phase in the petrochemical[1], pharmaceutical[2], desalination[3] and food processing[4] industries. Recent years have seen a rapid increase in the development of multifunctional porous materials that can be used to manufacture new membranes for separation of mixtures. These include, but not limited to, porous coordination polymers[5], nanoporous carbons[6] as well as polymers with intrinsic microporosity[7].

Different molecular modelling methods have been employed to study the separation of mixtures in porous membranes. One approach that has been commonly used is based on the solution-diffusion model.[8] In this approach permeability of a fluid, π_i, through a membrane is expressed as the product of the sorption coefficient, K_i, and the diffusion coefficient, D_i, that is, $\pi_i = K_i \times D_i$.[9] The sorption coefficient, K_i, is predicted by grand canonical Monte Carlo (GCMC) simulations, and the diffusion coefficient, D_i, is predicted by equilibrium molecular dynamics (EMD) simulations, hence this is often referred to as the GCMC+EMD approach. The ratio of the computed permeabilites are then used to calculate the permselectivity to characterize the performance of a membrane material for a specific separation. On the other hand, the solution-diffusion model is based on several assumptions, and one implicit assumption is that the molar volumes of the fluid in the membrane phase and in the bulk phases are equal[10]. Therefore, the permselectivity predicted by the GCMC+EMD approach is expected to be more reliable at conditions where components of the mixture do not interact strongly, i.e. at relatively low pressures. Furthermore, GCMC+EMD approach involves calculations made in periodic continuous structures, neglecting potential mass transfer resistance at the surface of the membranes.

Permeation of the components of a fluid mixture through membranes is a non-equilibrium process facilitated by the difference in the chemical potentials of the components at the inlet and outlet of a membrane; i.e. due to differences in pressure, temperature and concentration. As such, various non-equilibrium molecular dynamics (NEMD) methods have been developed and used to study the permeation of fluids in membranes. One approach is the hybrid Monte Carlo (MC) and MD technique, such as the dual control volume grand canonical molecular dynamics (DCV-GCMD)[11] and the grand relaxation molecular dynamics (GRMD)[12]. These hybrid approaches use MC particle insertion and deletion moves in two separate control volumes at opposite sides of a membrane to create pressure and/or concentration differences and have been employed to perform NEMD simulations of permeation of pure gases[11, 13] and binary mixtures[14] in various porous membranes. One challenge though, as highlighted by Ható et al.[15], is to optimize the ratio of the MC steps (i.e. insertion/deletion) vs. MD steps in order to perform a stable simulation. But a more significant issue with such hybrid approaches is that the insertion of particles in control volumes can be inefficient when the target density of the fluid is high, e.g. gases at high pressure or liquids, since the possibility of the inserted particle overlapping with an existing particle is high.

Another common NEMD approach to study permeation of fluids is to facilitate fluid transport through a membrane either by pushing the molecules with an impermeable wall or by applying a constant force on molecules individually (steered MD). This method has been typically used to study water transport[16], but also for mixture separation[17] through membranes. However, there are two major drawbacks of such brute force approaches that render them inadequate for running steady-state membrane transport and/or mixture separation simulations. The first problem is the feed depletion issue whereby it is not possible to run a continuous simulation because the simulation terminates after all molecules are pushed into the membrane and there are no fluid molecules left in the bulk. The second issue is that it is not possible to maintain the

feed composition of a mixture using the brute force approaches. Because the concentration of the slow diffusing molecules will gradually increase in the bulk while the faster diffusing molecules go through the membrane, which is contrary to the experimental case of constant feed composition.

Recently we developed a new method, concentration gradient driven molecular dynamics (CGD-MD) which addresses the shortcomings of previously used NEMD methods for simulating the permeation of fluids and separation of mixtures in membranes[18]. This method uses self-adjusting bi-directional bias forces to control and maintain the composition and density of a mixture at the inlet and outlet of a membrane. This, in turn, creates a concentration gradient which drives the diffusion of molecules through the membrane, that is, unlike the other NEMD methods the fluid molecules are not forced to diffuse through the membrane. Since no walls are used, molecules are circulated back to the feed through the periodic boundary avoiding the feed depletion issue. Overall CGD-MD provides a platform for running truly steady-state and, in principle, infinitely long simulations of mixture separations in membranes.

Experiments which involve the separation of mixtures with more than two components are relatively rare compared to experiments of binary mixture separation or permeation of pure fluids. To the best of our knowledge, there have been only a few NEMD simulations of permeation of mixtures with three or more components[19]. Furthermore, there are only a small number of studies which used the GCMC+EMD method to simulate separation of mixtures with three or more components[20, 21, 22]. A robust molecular simulation approach for predicting the separation performance of membranes for multi-component mixtures can be a powerful tool for predicting the selectivity of membrane materials for a specific multi-component separation, as well as for understanding the complex transport phenomena of mixtures through porous membranes.

In this study, we used the CGD-MD method to simulate the separation of a ternary mixture in a porous membrane. For this purpose, we considered the commercial hydrogen production from syngas which involves separation of hydrogen from syngas. The syngas mainly consists of H_2, N_2 and CO_2, but also some unconverted or partly converted combustible components like CH_4, CO, and possibly components like H_2S, and Ar. The typical composition of syngas in mol% from air-blown auto-thermal reforming and water gas shift reactions is 44-49 % H_2, 17% CO_2 and 33-38 % N_2[23]. In general, the CO_2 and the other impurities are separated from H_2 in a purification unit. The typical inlet feed temperature and pressure for H_2 purification unit are 300 K and 20-35 atm, respectively[23]. We used the reported composition and operating conditions to study the separation of H_2 from a CO_2, H_2 and N_2 mixture using a ZIF-8 membrane. ZIF-8 is a porous network structure connected using organic linkers and metal ions. In ZIF-8 cavities, ~ 11.6 Å in diameter, are interconnected via six-ring windows (3.4 Å)[24]. In several experimental studies, the gas molecules (CH_4, N_2, C_2H_6 and C_3H_8) with kinetic diameters larger than the six-ring windows were observed to freely diffuse through the ZIF-8 network owing to the rotational flexibility of the ZIF-8 organic linkers[25]. To model ZIF-8 framework flexibility several force fields have been developed[26, 27-29].

2. Model and Methodology

2.1. CGD-MD simulation setup

In this study, we used the CGD-MD method[18] to study the separation of H_2 from a H_2, CO_2, N_2 mixture (representing the main components of the syngas mixture) in a ZIF-8 membrane. The construction of the ZIF-8 membrane with energetically stable surface terminations was explained in Semino et al.[30]. The dimensions of the ZIF-8 membrane are L_x=50.98 Å, L_y=48.06 Å and L_z=106.0 Å (see **Figure 1**).

Figure 1 shows the set up for the CGD-MD simulations. Briefly, The ZIF-8 membrane is positioned at the centre of the simulation box, which has the dimensions of 50.98 Å × 48.06 Å × 300 Å, in the x, y and z directions, respectively. To create a concentration gradient across the membrane using the CGD-MD method, two control regions have been defined at the inlet and outlet of the membrane, inlet control region (ICR) and outlet control region (OCR). Between the membrane and the control regions, there are transitions regions; inlet transition region (ITR) and the outlet transition region (OTR). The composition of the gas mixture in the control regions, ICR and OCR, was maintained by self-adjusting bias forces which act within the inlet force region (IFR) and the outlet force region (OFR). The force regions are located between the control regions and the fluid reservoir. These bias forces act in such a way that if the concentration of a given species in a control region is different than the target concentration, molecules of that species are moved into or out of the control region from or to the reservoir, respectively. A detailed explanation of the functional forms of the bias forces and how they work can be found in Ozcan et al.[18] We emphasize again that it is not the bias forces which drive the permeation process but it is the concentration gradient which is formed by the bias forces. All CGD-MD simulations were performed with LAMMPS simulation package[31], in the NVT ensemble. Ewald summation was used to compute the long-range electrostatic interactions and the Lennard-Jones (LJ) potential was used to represent the short-range van der Waals interactions. A cut-off distance of 14 Å was employed for the LJ potential and for the real part of the Ewald summation. A time step of 1 fs was employed and two separate Nosé-Hoover thermostats were used to maintain the temperatures of the gas mixture and the ZIF-8 membrane at 300K. Periodic boundary conditions were employed in all three directions. The CGD-MD simulations were performed for 150 ns. The atomistic trajectories were collected for every 1 ps and these atomistic trajectories were used to compute the average flux and density profiles for the last 50 ns of the simulations. A private version of PLUMED 2.2.2[32] was used to apply the bias forces, F_i^{IFR} and F_i^{OFR}, which act in the IFR and OFR, respectively, to maintain

the concentrations of the mixture components in ICR and OCR (**Figure 1**). The inlet and outlet force constants, F_i^{IFR} and F_i^{OFR}, for CO_2, H_2 and N_2 molecules were 15000 and 50000 kJ nm^3/mol, respectively. The widths of ICR, OCR, ITR and OTR regions were 2 nm. The width of IFR and OFR regions were 0.25 nm.

The target inlet concentrations in ICR were set on the basis of typical syngas composition[23] at 35 bar total feed pressure and 300 K temperature, and were 297.24, 659.74 and 492.85 mol/m^3 for CO_2, H_2 and N_2, respectively. Based on density data from the NIST database[33] corresponding to mole fractions for CO_2, H_2 and N_2 in the mixture were 0.205, 0.455, and 0.340, respectively. The outlet concentration of the molecules in OCR were set to zero in order to create a vacuum effect on the outlet side of the membrane.

The flexibility of the membrane can affect the transport behaviour of the molecules, thus, four different flexible force-fields were considered to account for the ZIF-8 framework flexibility. These force fields are Zhang et al.[29], Semino et al.[30], Wu et al.[27] and Krokidas et al.[28]. In the Zhang et al.[29], Wu et al.[27] and Krokidas et al.[28] force fields, partial atomic charges and bonding parameters for surface atoms were not present since they were originally developed to study periodic ZIF-8 structures. Only Semino et al.[30] force-field included explicit representation of surface atoms, and partial charges of the surface atoms were calculated using DFT calculations. Therefore, for the Zhang et al.[29], Wu et al.[27] and Krokidas et al.[28] force fields, atomic charges of the surface atoms were scaled with respect to the framework atoms to get same surface charge ratio as presented in Semino et al..[30] Furthermore, bonding parameters, for the connectivity established by atoms attached on the surface were also taken from Semino et al..[30] H_2 molecule was represented with a three site model[34], and N_2 and CO_2 molecules were represented by parameters taken from the TraPPE force field.[35]

In order to estimate the number of gas molecules to be included in the CGD-MD simulation setup, Monte Carlo simulations in the grand canonical ensemble were carried out at 300 K and 35 atm using the RASPA molecular simulation package.[36] Details of the GCMC simulations are provided in the Supporting Information.

2. Results and Discussion

For a realistic simulation of H_2 separation from syngas using a membrane, it is important to reproduce the actual feed composition at experimentally relevant conditions. **Figure 2** shows the variation of CO_2, H_2 and N_2 concentrations in the inlet and outlet control regions (ICR and OCR, respectively) as a function of simulation time using four different ZIF-8 force fields. In all cases, the inlet concentrations of the gas molecules are stable and fluctuate around their average values, that is, syngas feed composition is maintained with very good accuracy with the CGD-MD approach. Similarly, at the outlet control region, the concentration remains very close to vacuum during the entire simulations. Simulated mole fractions of CO_2, H_2 and N_2 in the feed (i.e. ICR) agree very well with the target mole fractions established based on experimental conditions[23] (**Table S1**). The maximum deviation from the inlet target mole fractions is less than 6%.

The syngas composition maintained at the inlet of the ZIF-8 membrane and the vacuum maintained at the outlet of the ZIF-8 membrane create a concentration gradient which drives the permeation of gases through the membrane. The effect of such a gradient are apparent by the variation of the density of CO_2, H_2 and N_2 along the z-direction of the membrane as shown in **Figure 3**. The density of the gas molecules decreases gradually along the membrane. The peaks in density profiles correspond to the molecules adsorbed in the ZIF-8 cavities. Statistical errors in the z-density density profiles (**Figures S1, S2, S3** and **S4**) were found to be negligible and confirm that steady state has been achieved and flux can be calculated.

The flux of gas molecules through the ZIF-8 membrane,J_z, was calculated by counting the net number of molecules crossing a plane perpendicular to the direction of the gas flow at the centre of the membrane, A_{xy}, per time, t, using the following equation;

$$J_z = \frac{N_i^+ - N_i^-}{tA_{xy}} \qquad (1)$$

where N_i^+ and N_i^+ denote the number of molecules i which crosses the plane at the centre of the membrane in the positive and negative z directions, respectively. **Table S2** shows the fluxes of CO_2, H_2 and N_2 obtained with the different ZIF-8 force-fields used. In all cases, the order of the flux of the gases is H_2> CO_2> N_2. This is in reverse order of the kinetic diameters of these molecules, i.e. H_2 (2.9 Å), CO_2 (3.3 Å) and N_2 (3.6 Å), which indicates the flux is largely dominated by the ZIF-8 pore apertures. The variation in H_2 and CO_2 fluxes are relatively modest with respect to the force field used, whereas, N_2 flux varies more significantly. This is due to the relatively larger size of N_2, making its diffusion through the narrow apertures of ZIF-8 rather more sensitive to the ZIF-8 force field parameters.

To characterize the H_2 separation performance of the ZIF-8 membrane, permeation selectivities (S) was calculated using the equation below;

$$S_{ij} = \frac{J_i}{J_k} \times \frac{\Delta C_k}{\Delta C_i} \qquad (2)$$

where ΔC_i and ΔC_k represent the concentration difference between the inlet and outlet of the membrane for gas i and k, respectively. The average concentrations in ICR and OCR were used to compute the ΔC for each gas.

Table 1 shows the ZIF-8 permeation selectivities for H_2/CO_2, H_2/N_2 and $H_2/(CO_2+N_2)$ obtained from CGD-MD simulations. In general, predicted selectivities are close to each other regardless of the force field used. One exception is the H_2/N_2 selectivity predicted for the Semino et al. force field which is 4-7 times larger than other H_2/N_2 selectivities reported in **Table 1**. This

large difference is due to the very low N_2 flux (**Table 1**) computed with this force field. Selectivities obtained from the CGD-MD simulations are consistent in showing that, regardless of the force field used, ZIF-8 membrane has a good H_2 selectivity over CO_2 and an excellent selectivity over N_2 at the syngas composition, temperature and pressure considered in our study.

We further investigated how the selectivity predictions from CGD-MD simulations of H_2 separation from syngas in ZIF-8 membrane compare to those obtained from the GCMC+EMD approach. As explained in the introduction section, in the GCMC+EMD approach the permselectivity of a membrane, S_{ij}, is predicted by taking the ratio of permeabilities of gas species *i* and *j* through the membrane, that is,

$$S_{ij} = \frac{\pi_i}{\pi_j} = \frac{K_i \times D_i}{K_j \times D_j} \qquad (3)$$

Here, the adsorption selectivities (K_i/K_j) were calculated by carrying out mixture GCMC simulations at 300 K and 35 atm (see **Table S3** for adsorbed amounts). Diffusion selectivities (D_i/D_j) were calculated by performing EMD simulations and computing the self-diffusion coefficients of CO_2, H_2 and N_2 molecules in the adsorbed mixture (see **Figure S5** and **Table S4** for mean-squared displacement plots and the self-diffusion coefficients). In **Table 2** permeation selectivities, S_{ij}, predicted by the mixture GCMC+EMD approach, are shown for the four different ZIF-8 force fields used. In all cases the selectivity of H_2/CO_2 is found to be less than unity, and that the H_2/N_2 selectivity is only slightly more than unity. These results are unrealistic and not in agreement with the experimental results and the results from our CGD-MD simulations. It is well established that ZIF-8 is H_2 selective over both CO_2 and N_2.[37] Here one can argue that the incorrect permselectivity predictions by the mixture GCMC+EMD approach can be due to the fact that self-diffusion coefficients rather than the thermodynamically corrected transport diffusion coefficients[38] were used when calculating the permselectivities. However, it has been shown that although there can be quantitative differences between these

two types of diffusion coefficients, the ratios of the diffusion coefficients (i.e. diffusion selectivity) remain almost the same for light gases.[39] Therefore, we deduce that GCMC+EMD approach may not be reliable considering that the conditions for the separation of H_2 from syngas with a ZIF-8 membrane (i.e. at 300 K and 35 atm) are beyond the applicability of the solution-diffusion model (see introduction).

Since the GCMC+EMD approach is expected to give more accurate predictions at low pressure, we also calculated the permselectivities at infinite dilution using the GCMC+EMD method. This is a widely used approach for large scale screening studies.[21, 22] The popularity of the calculation of permselectivities at infinite dilution in large-screening studies is due to the relatively short time required for computing the adsorption and diffusion selectivities. At infinite dilution, adsorption selectivity becomes the ratio of Henry's constants of the gas molecules. Henry's constants for CO_2, H_2, and N_2 were calculated in Monte Carlo simulations at 300 K using the Widom's insertion method[40] (**Table S5** for Henry's constants). To calculate the diffusion selectivity at infinite dilution, on the other hand, self-diffusivities of CO_2, H_2, and N_2 were computed in EMD simulations of ZIF-8 system containing 30 gas molecules of each species at 300 K by switching off the gas-gas interactions[22, 41] (see **Figure S6** and **Table S6** for MSD plots and self-diffusion coefficients, respectively). In **Table 3**, the permselectivities obtained using the GCMC+EMD approach at infinite dilution are shown for the four force fields considered. H_2/CO_2 selectivities obtained using this approach are rather inconsistent between the different force-fields used. For instance, with the GCMC+EMD approach at infinite dilution, ZIF-8 is predicted to show no selectivity for the H_2/CO_2 using Semino et al. and Krokidas et al. force-fields. Whereas, relatively more consistent H_2/CO_2 selectivities were obtained using CGD-MD simulations regardless of the force field used (**Table 1**). Further, H_2/N_2 selectivities predicted by the GCMC+EMD approach at infinite dilution are considerably smaller than selectivities obtained from the CGD-MD simulations. This is due to the fact that GCMC+EMD

approach at infinite dilution does not take the mixture composition and the pressure at which the separation is carried out into account, therefore, it is only sensitive to the guest-host interactions. Improved predictions; however, may be obtained by employing the Maxwell Stefan (MS) formalism[42], which considers a balance between the chemical potential gradient and inter molecular frictional forces.

3. Conclusions

In this study, CGD-MD simulations were carried out to study the separation of H_2 from syngas in a ZIF-8 membrane at 300 K and 35 atm. In these simulations the concentrations of CO_2, H_2 and N_2 in the feed were maintained with excellent accuracy to maintain the feed composition at the target value. Four different force-fields were used to model the membrane flexibility, and regardless of the force-field used, permselectivities predicted by the CGD-MD approach showed that ZIF-8 is H_2 selective over CO_2 and N_2. On the other hand, H_2 permselectivities predicted by the GCMC+EMD approach for the separation of from syngas mixture in the ZIF-8 membrane were found to be incorrectly showing reverse selectivity. Overall, our results suggest that in order to accurately predict the permselectivity of a membrane for a multicomponent mixture separation at moderate or high pressure, a reliable NEMD approach, such as the CGD-MD method, should be employed.

Supporting Information

Average mole fractions attained in the inlet control region (ICR), fluxes obtained using different force fields from CGD-MD simulations, EMD based MSD plots obtained from the mixture and infinite dilution simulations, CO_2, H_2 and N_2 adsorption amounts and Henry's constants in ZIF-8 obtained from GCMC simulations, and z-density profiles of CO_2, H_2 and N_2 in ZIF-8 with error bars.

Acknowledgements

The authors would like to thank Dr Naseem Ramsahye, Dr Rocio Semino and Prof Guillaume Maurin for providing the ZIF-8 slab structure. This work has been funded by the Leverhulme

Trust Project Grant RPG-2016-331. We are grateful to the UK Materials and Molecular Modelling Hub for computational resources, which is partially funded by EPSRC (EP/P020194/1).

Received: ((will be filled in by the editorial staff))
Revised: ((will be filled in by the editorial staff))
Published online: ((will be filled in by the editorial staff))

References

[1] B. Van de Voorde, B. Bueken, J. Denayer, D. De Vos, Chem. Soc. Rev. 2014, 43, 5766; R.-B. Lin, L. Li, H.-L. Zhou, H. Wu, C. He, S. Li, R. Krishna, J. Li, W. Zhou, B. Chen, Nat. Mater. 2018, 17, 1128; H. Liu, Y. Pan, B. Liu, C. Sun, P. Guo, X. Gao, L. Yang, Q. Ma, G. Chen, Sci. Rep. 2016, 6, 21114; J. E. Bachman, Z. P. Smith, T. Li, T. Xu, J. R. Long, Nat. Mater. 2016, 15, 845.
[2] R. Xie, L.-Y. Chu, J.-G. Deng, Chem. Soc. Rev. 2008, 37, 1243; J. Imbrogno, L. Rogers, D. A. Thomas, K. F. Jensen, Chem. Comm. 2018, 54, 70; M. G. Buonomenna, J. Bae, Sep. Purif. Rev. 2015, 44, 157.
[3] J. R. Werber, C. O. Osuji, M. Elimelech, Nat. Rev. Mater. 2016, 1, 16018; G. Liu, W. Jin, N. Xu, Chem. Soc. Rev. 2015, 44, 5016.
[4] M. A. Augustin, Y. Hemar, Chem. Soc. Rev. 2009, 38, 902; B. Girard, L. R. Fukumoto, Crit. Rev. Food Sci. Nutr. 2000, 40, 91; V. Sant'Anna, L. D. F. Marczak, I. C. Tessaro, J. Food Eng. 2012, 111, 483.
[5] M. L. Foo, R. Matsuda, S. Kitagawa, Chemistry of Materials 2014, 26, 310.
[6] M. R. Benzigar, S. N. Talapaneni, S. Joseph, K. Ramadass, G. Singh, J. Scaranto, U. Ravon, K. Al-Bahily, A. Vinu, Chem. Soc. Rev. 2018, 47, 2680.
[7] N. B. McKeown, P. M. Budd, Chem. Soc. Rev. 2006, 35, 675.
[8] R. E. Lacey, S. Loeb, *Industrial processing with membranes*, Wiley-Interscience, New York 1972; J. G. Wijmans, R. W. Baker, J. Membr. Sci. 1995, 107, 1.
[9] C. H. Lee, J. Appl. Polym. Sci. 1975, 19, 83.
[10] J. G. Wijmans, J. Membr. Sci. 2004, 237, 39.
[11] G. S. Heffelfinger, F. v. Swol, J. Chem. Phys. 1994, 100, 7548.
[12] E. J. Maginn, A. T. Bell, D. N. Theodorou, J. Phys. Chem. 1993, 97, 4173.
[13] D. M. Ford, G. S. Heffelfinger, Mol. Phys. 1998, 94, 673; J. M. D. MacElroy, J. Chem. Phys. 1994, 101, 5274; R. F. Cracknell, D. Nicholson, N. Quirke, Phys. Rev. Lett. 1995, 74, 2463.
[14] L. Xu, M. G. Sedigh, M. Sahimi, T. T. Tsotsis, Phys. Rev. Lett. 1998, 80, 3511; L. Xu, T. T. Tsotsis, M. Sahimi, J. Chem. Phys. 1999, 111, 3252.
[15] Z. Ható, Á. Kaviczki, T. Kristóf, Mol. Simul. 2016, 42, 71.
[16] L. Wang, R. S. Dumont, J. M. Dickson, J. Chem. Phys. 2013, 138, 124701; L. Wang, R. S. Dumont, J. M. Dickson, RSC Adv. 2016, 6, 63586; M. Shen, S. Keten, R. M. Lueptow, J. Membr. Sci. 2016, 506, 95; K. M. Gupta, K. Zhang, J. Jiang, Langmuir 2015, 31, 13230.
[17] S. Velioglu, S. Keskin, J. Mater. Chem. A 2019, 7, 2301; K. M. Gupta, Q. Shi, L. Sarkisov, J. Jiang, J. Phys. Chem. C 2017, 121, 20539; S. Chen, A. Kucernak, J. Phys. Chem. B 2004, 108, 13984; C. Fang, H. Wu, S.-Y. Lee, R. L. Mahajan, R. Qiao, Carbon 2018, 136, 262; Y. Hou, Z. Xu, X. Yang, J. Phys. Chem. C 2016, 120, 4053; Q. Shi, Z. He, K. M. Gupta,

Y. Wang, R. Lu, J. Mater. Sci. 2017, 52, 173; W. Wei, K. M. Gupta, J. Liu, J. Jiang, ACS Appl. Mater. Interfaces 2018, 10, 33135.
[18] A. Ozcan, C. Perego, M. Salvalaglio, M. Parrinello, O. Yazaydin, Chem. Sci. 2017, 8, 3858.
[19] I. V. Kaganov, M. Sheintuch, Phys. Rev. E 2003, 68, 046701; L. Xu, M. G. Sedigh, T. T. Tsotsis, M. Sahimi, J. Chem. Phys. 1999, 112, 910; D. K. Dysthe, A. H. Fuchs, B. Rousseau, M. Durandeau, J. Chem. Phys. 1999, 110, 4060.
[20] I. Matito-Martos, A. Martin-Calvo, J. J. Gutiérrez-Sevillano, M. Haranczyk, M. Doblare, J. B. Parra, C. O. Ania, S. Calero, Phys. Chem. Chem. Phys. 2014, 16, 19884.
[21] H. Daglar, S. Keskin, J. Phys. Chem. C 2018, 122, 17347; Z. Qiao, Q. Xu, J. Jiang, J. Membr. Sci. 2018, 551, 47; G. Avci, S. Velioglu, S. Keskin, ACS Appl. Mater. Interfaces 2018, 10, 33693.
[22] Z. Qiao, C. Peng, J. Zhou, J. Jiang, J. Mater. Chem. A 2016, 4, 15904.
[23] M. C. Romano, P. Chiesa, G. Lozza, Int. J. Greenh. Gas Con. 2010, 4, 785; L. O. Nord, R. Anantharaman, O. Bolland, Int. J. Greenh. Gas Con. 2009, 3, 385.
[24] G. Férey, Chem. Soc. Rev. 2008, 37, 191.
[25] C. Gücüyener, J. van den Bergh, J. Gascon, F. Kapteijn, J. Am. Chem. Soc. 2010, 132, 17704; H. Bux, C. Chmelik, R. Krishna, J. Caro, J. Membr. Sci. 2011, 369, 284; H. Bux, C. Chmelik, J. M. van Baten, R. Krishna, J. Caro, Adv. Mater. 2010, 22, 4741; K. Li, D. H. Olson, J. Seidel, T. J. Emge, H. Gong, H. Zeng, J. Li, J. Am. Chem. Soc. 2009, 131, 10368; E. H. Fort, P. M. Donovan, L. T. Scott, J. Am. Chem. Soc. 2009, 131, 16006.
[26] B. Zheng, M. Sant, P. Demontis, G. B. Suffritti, J. Phys. Chem. C 2012, 116, 933; L. Hertäg, H. Bux, J. Caro, C. Chmelik, T. Remsungnen, M. Knauth, S. Fritzsche, J. Membr. Sci. 2011, 377, 36; Z. Hu, L. Zhang, J. Jiang, J. Chem. Phys. 2012, 136, 244703.
[27] X. Wu, J. Huang, W. Cai, M. Jaroniec, RSC Adv. 2014, 4, 16503.
[28] P. Krokidas, M. Castier, S. Moncho, E. Brothers, I. G. Economou, J. Phys. Chem. C 2015, 119, 27028.
[29] L. Zhang, Z. Hu, J. Jiang, J. Am. Chem. Soc. 2013, 135, 3722.
[30] R. Semino, N. A. Ramsahye, A. Ghoufi, G. Maurin, ACS Appl. Mater. Interfaces 2016, 8, 809.
[31] S. Plimpton, J. Comput. Phys. 1995, 117, 1.
[32] G. A. Tribello, M. Bonomi, D. Branduardi, C. Camilloni, G. Bussi, Comput. Phys. Commun. 2014, 185, 604.
[33] E. W. Lemmon, M. O. McLinden, D. G. Friend, *Thermophysical Properties of Fluid Systems*, NIST Chemistry WebBook, NIST Standard Reference Database Number 69 National Institute of Standards and Technology, Gaithersburg MD, 20899.
[34] J. J. Potoff, J. I. Siepmann, AIChE J 2001, 47, 1676.
[35] F. Darkrim, D. Levesque, J. Chem. Phys. 1998, 109, 4981.
[36] D. Dubbeldam, S. Calero, D. E. Ellis, R. Q. Snurr, Mol. Simul. 2016, 42, 81.
[37] Y. Pan, Z. Lai, Chem. Comm. 2011, 47, 10275.
[38] K. Zhang, R. P. Lively, C. Zhang, R. R. Chance, W. J. Koros, D. S. Sholl, S. Nair, J. Phys. Chem. Lett. 2013, 4, 3618.
[39] A. I. Skoulidas, D. S. Sholl, J. Phys. Chem. B 2005, 109, 15760.
[40] J. M. Castillo, D. Dubbeldam, T. J. H. Vlugt, B. Smit, S. Calero, Mol. Simul. 2009, 35, 1067.
[41] C. Altintas, G. Avci, H. Daglar, E. Gulcay, I. Erucar, S. Keskin, J. Mater. Chem. A 2018, 6, 5836.
[42] H. Strathmann, AIChE J 2001, 47, 1077; D. S. Sholl, Acc. Chem. Res. 2006, 39, 403.

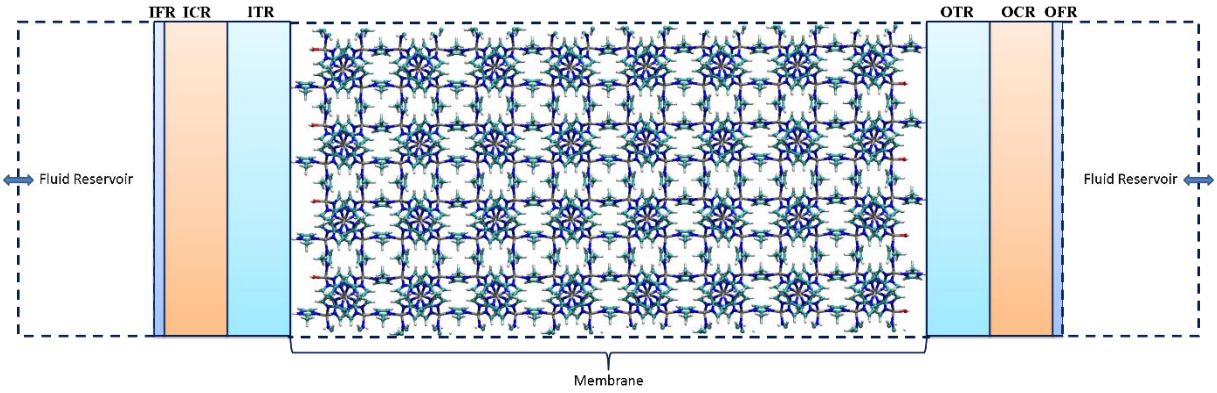

Figure 1. Schematic representation of the model simulation system and the CGD-MD method. The feed side and permeate side fluid molecules are free to move from one side to the other side through the periodic boundary (shown with two-way arrows).

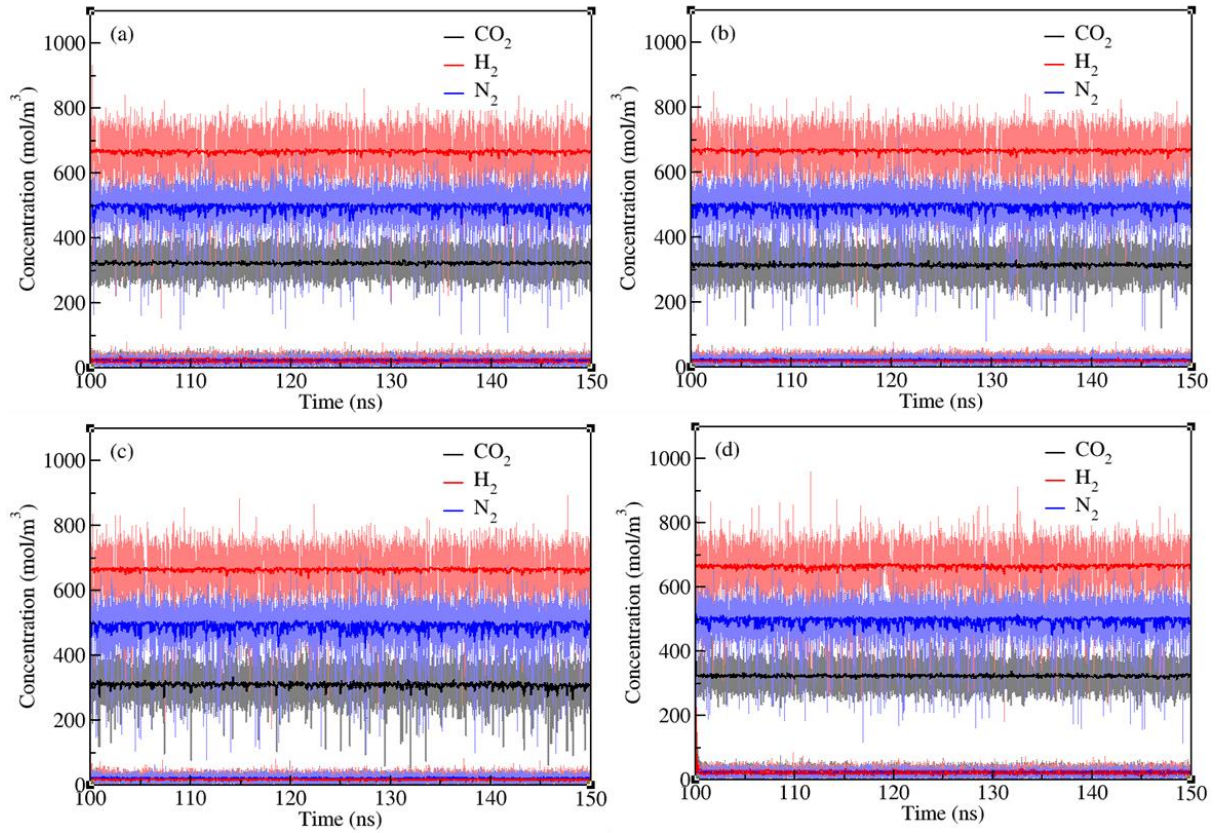

Figure 2. The concentrations of CO_2 (black lines) H_2 (red lines) and N_2 (blues lines) as a function of time in the ICR and OCR of CGD-MD simulations of ZIF-8 membrane separation using (a) Semino et al. (b) Wu et al. (c) Zhang et al. and (d) Krokidas et al. force fields. The instantaneous values of species concentration are shown in a light colour, while the moving averages obtained over a smoothing time of 0.2 ns are shown as full-colour curves.

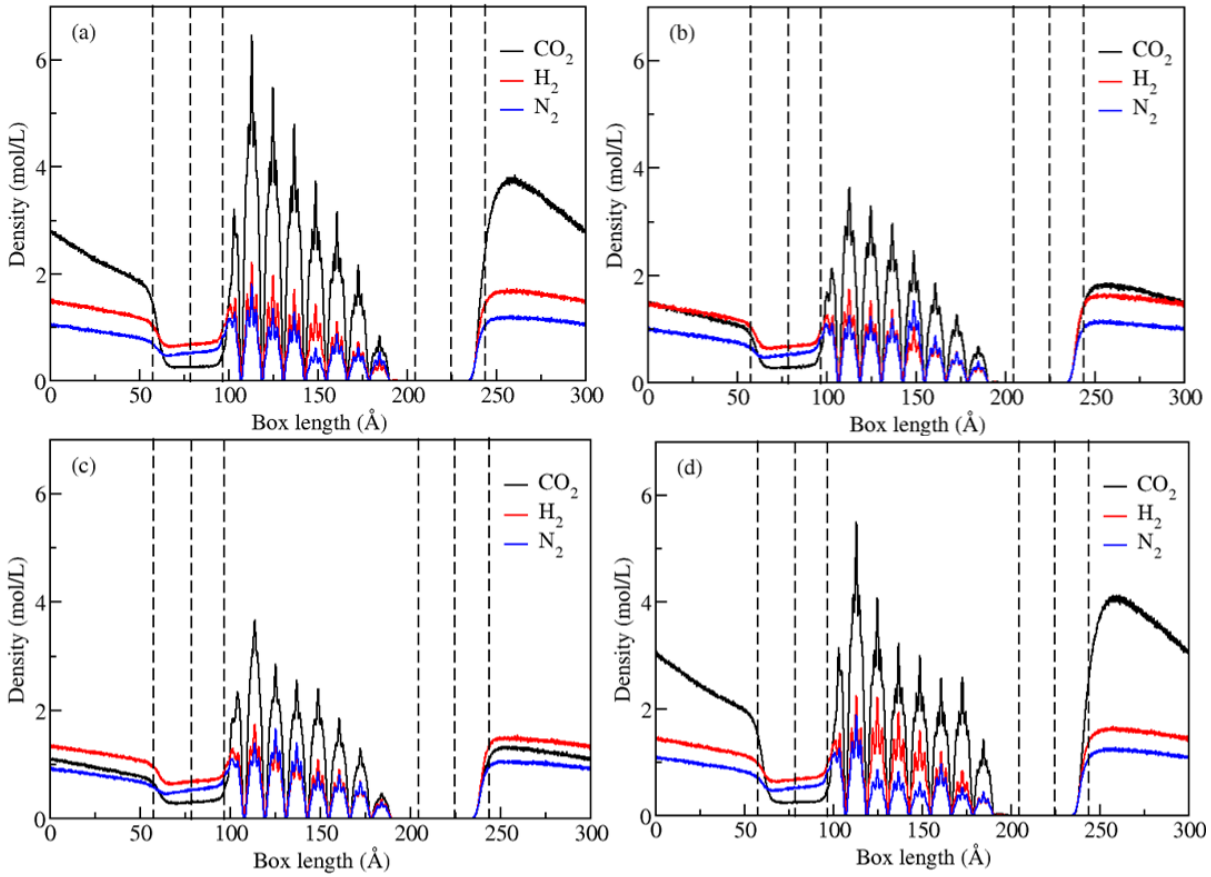

Figure 3. The density profiles of CO_2, H_2, and N_2 molecules in the direction of flow (z) obtained in CGD-MD simulations of ZIF-8 membrane separation obtained with using (a) Semino et al. (b) Wu et al. (c) Zhang et al. and (d) Krokidas et al., force-fields. The regions between the dashed vertical lines represent the ICR (58-78 Å), ITR (78-98 Å), Membrane (98-204), OTR (204-224 Å), and OCR (224-244). See **Figure 1** for the definitions of ITR, OTR, ICR and OCR.

Table 1. Permselectivities based on gas fluxes calculated from the CGD-MD simulations for four different ZIF-8 force fields.

	Semino et al.	**Wu et al.**	**Zhang et al.**	**Krokidas et al.**
H_2/CO_2	7.4	5.4	6.3	11.2
H_2/N_2	478.3	71.6	111.6	89.6
$H_2/(CO_2+N_2)$	18.87	12.61	24.01	15.26

Table 2. Permselectivities obtained from the mixture GCMC+EMD approach for four different ZIF-8 force fields.

	Semino et al.	**Wu et al.**	**Zhang et al.**	**Krokidas et al.**
H_2/CO_2	0.13	0.21	0.26	0.17
H_2/N_2	1.68	1.20	1.23	1.64

Table 3. Permselectivities obtained from the infinite dilution GCMC+EMD approach for four different ZIF-8 force fields.

	Semino et al.	**Wu et al.**	**Zhang et al.**	**Krokidas et al.**
H_2/CO_2	0.98	4.84	2.29	0.88
H_2/N_2	4.95	11.02	8.80	3.44

The table of contents entry:

Non-equilibrium molecular dynamics (NEMD) simulations of membrane separation of a ternary mixture at high pressure is carried out by using the concentration gradient driven molecular dynamics (CGD-MD) method. While the permselectivities obtained with the CGD-MD method are found to be accurate, permselectivities obtained by using the grand canonical Monte Carlo + equilibrium molecular dynamics (GCMC+EMD) approach are found to be incorrect.

S. Namsani, A. Ozcan and A. O. Yazaydin*

Direct simulation of ternary mixture separation in a ZIF-8 membrane at molecular scale

ToC figure